

1 Supplementary Information

## 2 **Supplementary Methods**

### 4 ***Protein purification***

5 Truncated H1.3 coding 37-211 ( $\Delta$ N) and 1-111 amino acids ( $\Delta$ C) were expressed  
6 and purified as described elsewhere (1).

### 8 ***The affinity between HP1 $\gamma$ and histone H3N-terminal peptides***

9 The affinities of HP1 $\gamma$  and the CD domain towards the N-terminal tail peptide  
10 (1-19) of H3 were determined by ITC as described previously (2). The N-terminal  
11 peptide of H3 (1-19) containing H3cK9me3, in which lysine residue was replaced  
12 with aminoethyl cysteine, was prepared as described (2). In brief, histone H3  
13 (1-19) carrying K9C mutation was expressed with SUMO-tag in bacteria. The  
14 fusion protein was digested with SENP2 protease, and the peptide was purified  
15 with reverse phase chromatography. The unmodified or trimethylated lysine  
16 analogue was introduced into the peptide as described (3).

### 18 ***Gel shift assays***

19 GST, GST- HP1 $\gamma$ , GST- HP1 $\gamma$  CD+HR, GST- HP1 $\gamma$  CD, GST-HP1 $\alpha$  CD+HR,  
20 GST- HP1 $\alpha$  CD, and GST-HP1 $\gamma$ - $\alpha$ HR (1, 4, and 8  $\mu$ M) was mixed with 25 nM of  
21 monosomal DNA without linker, of length 147bp, described by Mishima *et al.*  
22 (2), in the binding buffer including 100 mM NaCl and the binding activity was  
23 determined as described in the Materials and Methods. To examine the  
24 interaction between GST-HP1 $\gamma$  and DNA in the presence of MgCl<sub>2</sub>, 3 mM  
25 MgCl<sub>2</sub>, instead of EDTA, was added in the binding buffer including 100 mM  
26 NaCl, and separated in a 0.7% agarose gel in 45 mM Tris-borate, and 3 mM  
27 MgCl<sub>2</sub>.

### 28 ***MgCl<sub>2</sub>-dependent nucleosome precipitation***

29 Nucleosomes were precipitated by centrifugation in the presence of MgCl<sub>2</sub> (4, 5).  
30 In brief, 40 ng DNA/ $\mu$ l tetra-nucleosomes or mono-nucleosomes in buffer B  
31 comprising 2.5 mM NaCl, 0.25 mM EDTA, 10 mM Tris-HCl, pH 7.8 were mixed  
32 with an equal volume of buffer B containing MgCl<sub>2</sub> to make the indicated final  
33 MgCl<sub>2</sub> concentrations. After the incubation at room temperature for 10 min,  
34 samples were centrifuged at 10,000 x g for 10 min at room temperature. The  
35 absorbance at 260 nm of the supernatant fraction, which was not precipitated,  
36 was determined in a Nanodrop (Thermo Fisher Scientific, Inc).

37

38 ***Gel filtration***

39 Purified HP1 without GST tag was separated by size exclusion chromatography,  
40 as described in Materials and Methods, with slight modification. The buffer used  
41 contained either 0.2 mM EDTA or 3 mM MgCl<sub>2</sub>.

42

43 ***MgCl<sub>2</sub>-dependent binding of HP1 $\gamma$  to tetra-nucleosomes***

44 To analyze the interaction between HP1 $\gamma$  and reconstituted nucleosomes, 0.2  
45 nM HP1 $\gamma$  and 90 nM of tetra-nucleosomes (amount converted to that of a  
46 nucleosome particle with a histone octamer) were mixed in 10  $\mu$ l of binding  
47 buffer containing 6 mM MgCl<sub>2</sub>, incubated at room temperature for 30 min, and  
48 then centrifuged at 10,000 x g for 10 min at 4°C. The supernatant and  
49 precipitated fractions were separately electrophoresed in an 18% SDS-  
50 polyacrylamide gel. The protein bands were transferred onto a nitrocellulose  
51 membrane, and the HP1 $\gamma$  and H4 were immuno-detected with the specific  
52 antibodies.

53

54 ***Pull down assay determining nucleosome-binding activity of HP1 $\alpha$***

55 Pull down assay was performed as described in Materials and Methods. Two or  
56 four pmol (amount converted to that of a nucleosome particle with a histone  
57 octamer) of reconstituted nucleosomes were incubated with 40 or 80 pmol of  
58 GST- HP1 $\alpha$ -bound GSH-Sepharose, unless otherwise mentioned.

59

60 ***H1-dependent nucleosome precipitation***

61 Tetra-nucleosomes (0.2  $\mu$ M, amount converted to that of a nucleosome particle  
62 with a histone octamer) were incubated with 0.8  $\mu$ M H1 in the binding buffer, and  
63 centrifuged at 10,000 x g for 1 min at 4°C. As a control, 0.5  $\mu$ M HP1 $\gamma$ , I155K, or  
64 the CD, or 0.8  $\mu$ M H1 alone was centrifuged. The supernatant and precipitated  
65 fractions were electrophoresed in an 18% SDS-polyacrylamide gel, and stained  
66 with Lumitein.

67

68 ***Pull-down assay in the presence of H1***

69 Pull-down assays were performed as described in the Materials and Methods,  
70 except for fixed amount of H1 (four molar excess amount converted to that of a  
71 nucleosome particle with a histone octamer) was added to the reaction mixture.

72 **Legends for Supplementary Figures**

73 **Supplementary Figure S1. Affinity of HP1 $\gamma$  to the N-terminal peptide of H3.**

74 ITC titration curves of full-length HP1 $\gamma$  (FL) (A) and the CD of HP1 $\gamma$  coding  
75 (1-75) (CD) (B) towards the N-terminal peptide of histone H3 (1-19) containing  
76 lysine analogue at K9 with tri-methylated (H3cK9me3) (left panel) or  
77 unmethylated (H3cK9me0) (right panels) are shown. (C) The dissociation  
78 constants are calculated by fitting the data using the ITC data analysis module of  
79 Origin 7.0 (OriginLab, Northampton, MA). The dissociation constants are shown  
80 in  $\mu$ M. Measurements below the detection limit are indicated as b.d. The  
81 dissociation constants for HP1 $\alpha$  (\*) are taken from a previous report (2).

82

83 **Supplementary Figure S2. HP1 $\alpha$ , HP1 $\gamma$ , and H1 isoforms used in the**  
84 **present study.**

85 (A) Amino acid sequences of human HP1 $\alpha$  and HP1 $\gamma$  aligned with ClustalW  
86 (<http://clustalw.ddbj.nig.ac.jp/>). The CD, HR, and CSD are indicated in light blue,  
87 dark blue, and red, respectively. Identical amino acids are indicated as asterisks  
88 below the alignment. Colon and dot indicate similar and less similar amino  
89 acids, respectively. Ile 165 in HP1 $\alpha$ , which is reported to be crucial for  
90 dimerization (6), is enclosed with red square. Ile 155 in HP1 $\gamma$  is the  
91 corresponding residue to the Ile 155 in HP1 $\alpha$ . (B) SDS-polyacrylamide gel  
92 electrophoresis of purified HP1 $\alpha$ , HP1 $\gamma$ , and H1 isoforms. Recombinant GST,  
93 GST-tagged wild-type, truncated and mutant HP1 $\alpha$ , HP1 $\gamma$ , and their chimera  
94 HP1 (upper left panel), HP1 $\alpha$ , HP1 $\gamma$ , HP1 $\alpha$  I165K, HP1 $\gamma$  I155K, and HP1 $\gamma$ (1-75)  
95 (upper right panel), wild type H1.2, H1.3, H1.4, and H1.5 (lower left panel), and  
96 the N- and C-terminal truncated H1.3 (lower right panel) (0.5  $\mu$ g each) were  
97 separated in 18% SDS-polyacrylamide gels, and stained with Coomassie  
98 Brilliant Blue (CBB). Molecular size markers are indicated at left of each panel.

99

100 **Supplementary Figure S3. DNA binding activity of GST-HP1 $\gamma$  and GST-**  
101 **HP1 $\alpha$ .**

102 (A) Naked DNA was incubated without protein (lane 1), with GST-HP1 $\alpha$  (lanes  
103 2-4), GST- HP1 $\gamma$  (lanes 5-7), GST-HP1 $\gamma$ - $\alpha$ HR (lanes 8-10) or GST (lanes  
104 11-13). To DNA, 40 (lanes 2, 5, 8 and 11), 160 (lanes 3, 6, 9 and 12), or 320  
105 (lanes 4, 7, 10 and 13) molar excess of protein was added, and the binding  
106 activity was examined as described in **Figure 3A**. (B) Naked DNA was  
107 incubated without (lane 1) or with GST-HP1 $\gamma$  (lanes 2-4). To the DNA, 40 (lane  
2), 160 (lane 3), or

108 320 (lane 4) molar excess of GST-HP1 $\gamma$  was added in the presence of 3 mM  
109 MgCl<sub>2</sub>, and the reaction mixture was separated in a 0.7% agarose containing 45  
110 mM Tris-borate, and 3 mM MgCl<sub>2</sub>. Arrowhead and bracket indicate the position  
111 of free DNA and shifted DNA, respectively.

112

113 **Supplementary Figure S4. The CSD of GSTHP1 $\gamma$  negatively regulates the**  
114 **binding to DNA.**

115 **(A)** Schematic illustration of truncated GST-HP1 $\gamma$ . **(B)** The binding of tetra-  
116 nucleosomes to the GST-HP1 $\gamma$  deleted the HR and/or the CSD was determined  
117 as described in **Figure 1C**. The GSH-Sepharose bound with the truncated GST-  
118 HP1 $\gamma$  was incubated with unmethylated H3 (unme) or H3K9me3 (K9me3) tetra-  
119 nucleosomes (left panel). The relative amounts of core histones recovered in  
120 the bound fraction over the input (%) were calculated and shown as mean  $\pm$  S.  
121 E. (n=3) (right panel). **(C)** Naked DNA was incubated without protein (lane 1),  
122 with GST-HP1 $\alpha$ FL (lanes 2-4), GST-HP1 $\alpha$ CD+HR (lanes 5-7), GST-  
123 HP1 $\alpha$ CD (lanes 8-10), GST-HP1 $\gamma$  (lanes 11-13), GST-HP1 $\gamma$ CD+HR (lanes  
124 14-16), or GST-HP1 $\gamma$ CD (lanes 17-19). To the DNA, 40 (lanes 2, 5, 8, 11, 14  
125 and 17), 160 (lanes 3, 6, 9, 12, 15 and 18), or 320 (lanes 4, 7, 10, 13, 16 and  
126 19) molar excess of protein was added, and the binding activity was determined  
127 as described in **Figure 3A**. Arrowhead and bracket indicate the position of free  
128 DNA and shifted DNA, respectively.

129

130 **Supplementary Figure S5. Effect of MgCl<sub>2</sub> concentration on the**  
131 **aggregation state of tetra- and mono-nucleosomes.**

132 Unmethylated H3 (open circles) and H3K9me3 (closed circles) tetra- **(A)**, or  
133 mono-nucleosomes **(B)** were incubated with indicated concentrations of MgCl<sub>2</sub>,  
134 and then centrifuged. The absorbance at 260 nm of the input and supernatant  
135 fractions was determined, and ratio (%) of tetra- and mono-nucleosomes in the  
136 supernatant to the input is shown as mean  $\pm$  S. E. (n=3).

137

138 **Supplementary Figure S6. Effect of MgCl<sub>2</sub> on the elution profile of HP1 $\gamma$  on**  
139 **gel filtration.**

140 HP1 $\gamma$  whose GST-tag was removed was loaded onto a Superdex 200 column (1  
141 x 30 cm), equilibrated with a buffer containing either 0.2 mM EDTA (solid line) or  
142 presence of 3 mM MgCl<sub>2</sub> (dotted line). Absorbance at 280 nm was monitored.

143

144 **Supplementary Figure S7. MgCl<sub>2</sub> dependent interaction between HP1 $\gamma$  and**  
145 **tetra-nucleosomes.**

146 Unmethylated H3 (lanes 1, 2, 5, and 6) or H3K9me3 (lanes 3, 4, 7, and 8) tetra-  
147 nucleosomes were incubated with HP1 $\gamma$ , in the reaction buffer containing 50  
148 mM NaCl, either in the presence of 6 mM (lanes 1-4) or in the absence of MgCl<sub>2</sub>  
149 (lanes 5-8). After incubation, mixtures were centrifuged and then the  
150 supernatant (S) and precipitated (P) fractions were separately recovered.  
151 Histone H4 and HP1 $\gamma$  in the fractions were detected with Western blotting.

152

153 **Supplementary Figure S8. Binding activity of GST-HP1 $\alpha$  towards**  
154 **H3K9me3 tetra-nucleosomes in the presence or absence of MgCl<sub>2</sub>.**

155 Unmethylated or H3K9me3 tetra-nucleosomes, were incubated with GST-HP1 $\alpha$   
156 bound to GSH Sepharose, as described in either Figure 1C (in the absence of  
157 MgCl<sub>2</sub>) or Figure 2A, in the presence of 3 mM MgCl<sub>2</sub> and 50 mM NaCl. **(A)** Two  
158 pmol of reconstituted nucleosomes were incubated with 80 pmol of GST- HP1 $\gamma$ -  
159 bound GSH-Sepharose. The data for binding activity of HP1 $\alpha$  in the absence of  
160 MgCl<sub>2</sub> are taken from previous report (2) **(B)** Four pmol of reconstituted  
161 nucleosomes were incubated with 40 pmol of GST-HP1 $\gamma$ -bound GSH-  
162 Sepharose. The binding activity was quantitated as in Figure 1C. Means  $\pm$  S. E.  
163 (n=3) are shown.

164

165 **Supplementary Figure S9. Precipitation of tetra-nucleosomes in the**  
166 **presence of H1 isoforms.**

167 Unmethylated H3 (unme, lanes 1, 2, 5, 6, 9, 10, 13, 14, 17 and 18) or H3K9me3  
168 (K9me3, lanes 3, 4, 7, 8, 11, 12, 15, 16, 19 and 20) tetra-nucleosomes  
169 were incubated without (lane 1-4), or with H1.2 (lanes 5-8), H1.3 (lanes 9-12),  
170 H1.4 (lanes 13-16), or H1.5 (lanes 17-20). After the incubation, the reaction  
171 mixtures were centrifuged, and supernatant (S) and precipitated (P)  
172 fractions were separately recovered, and then electrophoresed in an 18%  
173 SDS-polyacrylamide gel. Arrow and bracket indicate H1 and core histones,  
174 respectively. Molecular size markers are shown at the left of the gel (kDa).

175

176 **Supplementary Figure S10. HP1 $\gamma$  or/and H1 does not form aggregation.**

177 HP1 $\gamma$  (WT) (lanes 1 and 2), HP1 $\gamma$  I155K (I155K) (lanes 3 and 4), HP1 $\gamma$  CD  
178 (lanes 5 and 6) (0.5  $\mu$ M), or 0.8  $\mu$ M of H1.2 (lanes 7 and 8), H1.3 (lanes 9 and  
179 10), H1.4 (lanes 11 and 12), or H1.5 (lanes 13 and 14) **(A)**, and a mixture

180 containing HP1 $\gamma$  (0.5  $\mu$ M) and H1 isoforms (0.8  $\mu$ M), H1.2 (lanes 1 and 2), H1.3  
181 (lanes 3 and 4), H1.4 (lanes 5 and 6), or H1.5 (lanes 7 and 8) **(B)** were  
182 centrifuged, supernatant (S) and precipitated (P) fractions were separately  
183 recovered, and then analyzed as in **Supplementary Figure S9**. Arrows and  
184 arrowheads indicate H1 isoforms and HP1 $\gamma$ , respectively. Molecular size  
185 markers (kDa) are shown at the left of images.

186

187 **Supplementary Figure S11. Binding of GST-HP1 $\gamma$  to H3K9me3 tetra-**  
188 **nucleosomes condensed by H1 isoforms.**

189 GST-HP1 $\gamma$  binding to tetra-nucleosomes condensed by H1 isoforms were  
190 examined as in **Figure 1C**. GSH-Sepharose, on which GST-HP1 $\gamma$  were  
191 anchored, was incubated with unmethylated H3 (unme) or H3K9me3 (K9me3)  
192 tetra-nucleosomes. After incubation, input (I), unbound (U), wash (W), and  
193 pulled down bound (B) fractions for H1.2, H1.3, H1.4, and H1.5 were separated.  
194 Core histones are indicated by brackets **(A)**. The relative amounts of core  
195 histones recovered in the bound fraction over the input (%) were calculated and  
196 shown as mean  $\pm$  S. E. (n=3) **(B)**.

197

198 **Supplementary Figure S12. Binding of GST-HP1 $\gamma$  with tetra-nucleosomes**  
199 **in the presence of truncated H1.3.**

200 **(A)** Schematic illustration of full-length (FL), the N-terminal deleted H1.3  
201 (37-221) ( $\Delta$ N), and C-terminal deleted H1.3  $\Delta$ C (1-111). Globular domains are  
202 indicated by ellipses. **(B)** Binding of truncated H1.3 to tetra-nucleosomes.  
203 Unmethylated H3 (unme, upper panel) or H3K9m3 (K9me3, lower panel) tetra-  
204 nucleosomes were incubated without H1 (lanes 1 and 10) or with H1.3  $\Delta$ N ( $\Delta$ N)  
205 (lanes 2-5 and 11-14), or H1.3  $\Delta$ C ( $\Delta$ C) (lanes 6-9 and 15-18). To 0.2 pmol of  
206 histone octamer, a half (lanes 2, 6, 11 and 15), equal (lanes 3, 7, 12 and 16),  
207 two-fold (lanes 4, 8, 13 and 17), or four-fold (lanes 5, 9, 14 and 18) molar  
208 excess of truncated H1.3 was added and electrophoresed. Tetra-nucleosomes  
209 and H1-bound fractions of tetra-nucleosomes are indicated by arrowheads and  
210 brackets, respectively. **(C)** Effect of truncated H1.3 on the binding of HP1 $\gamma$  to  
211 the tetra-nucleosomes (left panel). Bound over input (%) was determined and  
212 means  $\pm$  S. E. (n=3) are shown.

213

214 **Supplementary Figure S13. Whole gel images for the main figures.**

215 The regions excised are shown as red boxes. In panels for Figures 1A, 1C, 1G,

216 2A, 2C, 2E, 3B, 4A, and 4C, the input (one-fourth of each) (I), unbound (U),  
217 wash (W), and bound (B) fractions were electrophoresed. For the binding  
218 experiments, unmethylated H3 (unme) or H3K9me3 (K9me3) tetra-  
219 nucleosomes were used. The positions of GST, H3, H4, HP1 $\alpha$ , HP1 $\gamma$ , and H1  
220 isoforms are indicated in each corresponding images.  
221

222 **REFERENCES**

223

224 1, Takeshima, H., Suetake, I., and Tajima, S. (2008). Mouse Dnmt3a  
225 preferentially methylates linker DNA and is inhibited by histone H1. *J. Mol. Biol.*,  
226 **383**, 810-821.

227

228 2, Mishima, Y., Watanabe, M., Kawakami, T., Jayasinghe, C. D., Otani, J.,  
229 Kikugawa, Y., Shirakawa, M., Kimura, H., Nishimura, O., Aimoto, Tajima, S., and  
230 Suetake, I. (2013) Hinge and chromoshadow of HP1 $\alpha$  participate in recognition  
231 of K9 methylated histone H3 in nucleosomes. *J. Mol. Biol.*, **425**, 54-70.

232

233 3, Simon, M. D. (2010) Installation of site-specific methylation into histones using  
234 methyl lysine analogs. *Curr. Protoc. Mol. Biol. Chapt 21*: unit 21.18, pp. 1-10,  
235 John Wiley and Sons, Inc.

236

237 4, Schwarz, P. M and Hansen, J. C. (1994) Formation and Stability of Higher  
238 Order Chromatin Structures. *J. Biol. Chem.*, **269**, 16284-16289.

239

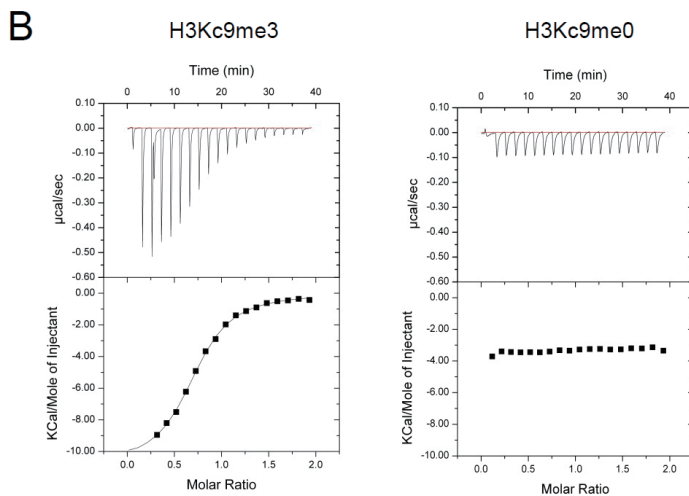
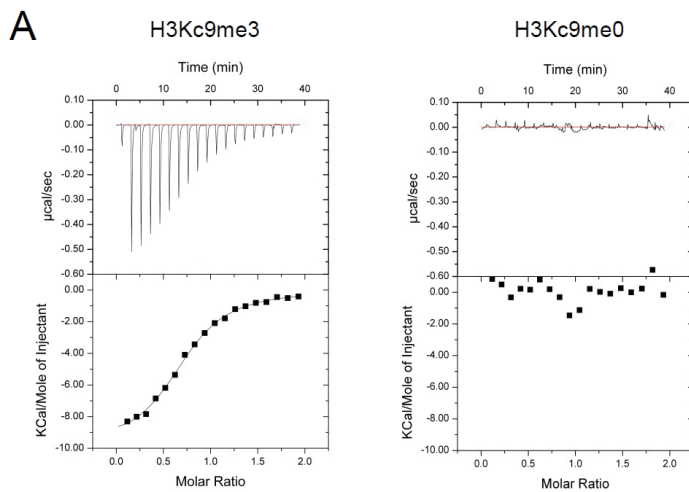
240 5, Blacketer, M. J., Feely, S. J., and Shogren-Knaak, M. A. (2010) Nucleosome  
241 Interactions and Stability in an Ordered Nucleosome Array Model System. *J. Biol.*  
242 *Chem.*, **285**, 34597-34607.

243

244 6, Lechner, M. S., Schultz, D. C., Negorev, D., Maul, G. G., and Rauscher, F. J.  
245 3rd. (2005) The mammalian heterochromatin protein 1 binds diverse nuclear  
246 proteins through a common motif that targets the chromoshadow domain.  
247 *Biochem. Biophys. Res. Commun.*, **331**, 929-937.

248

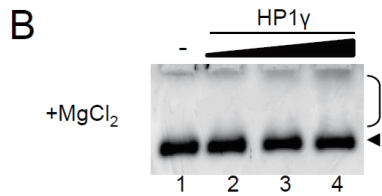
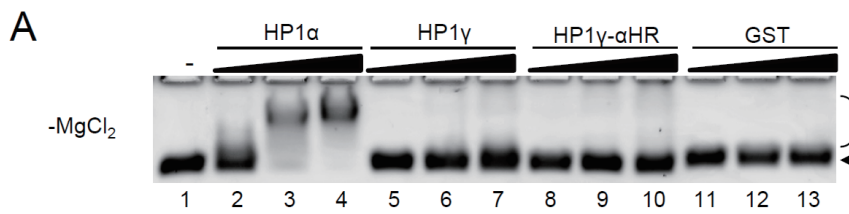
249



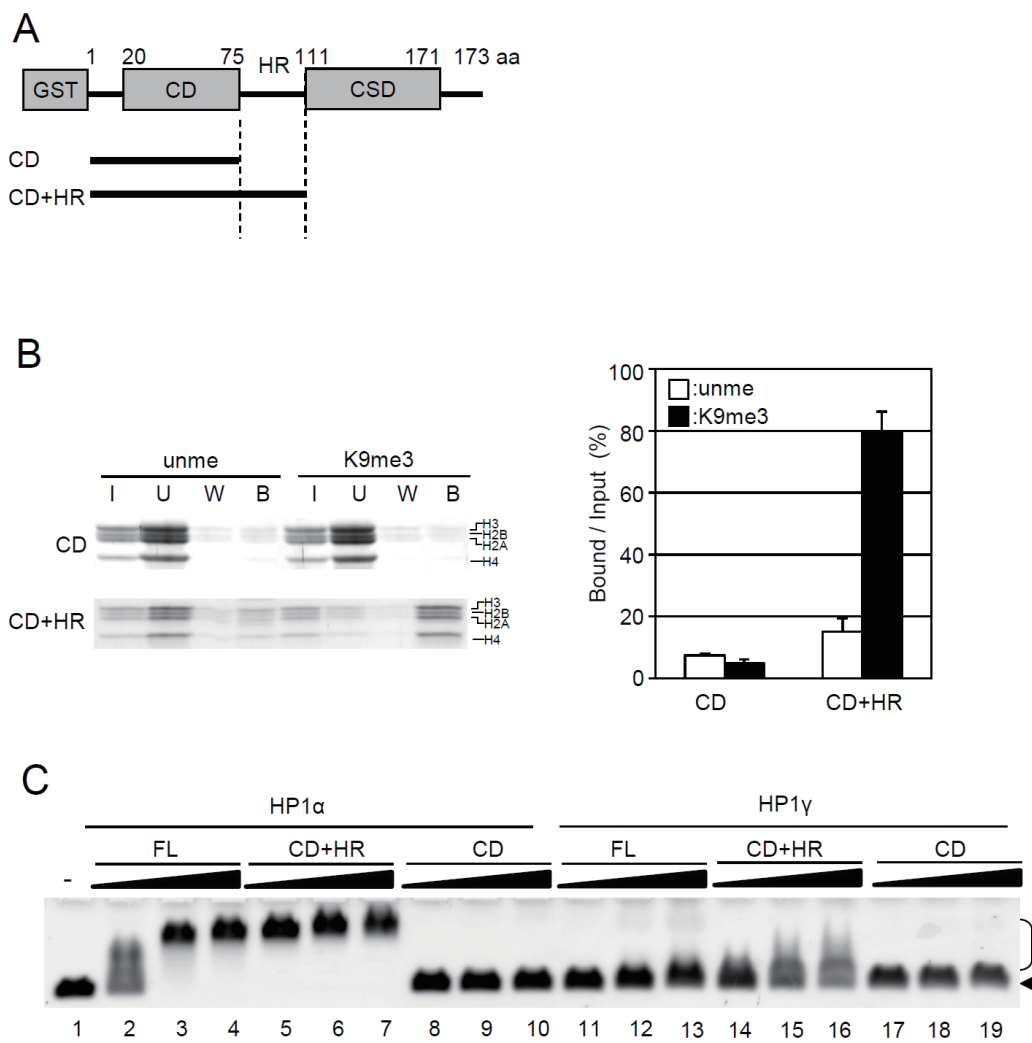
**C**

		H3Kc9me0	H3Kc9me3
HP1 $\alpha$	FL	b.d.	12*
	CD	b.d.	16*
HP1 $\gamma$	FL	b.d.	2.5
	CD	b.d.	3.9

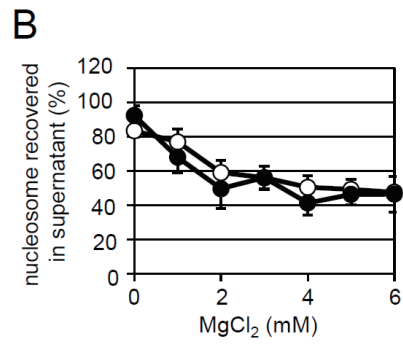
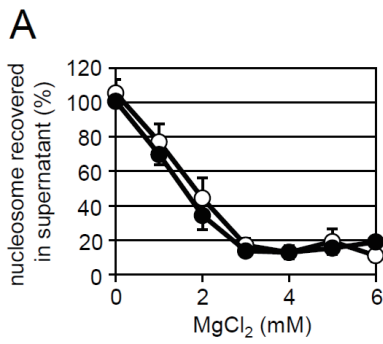




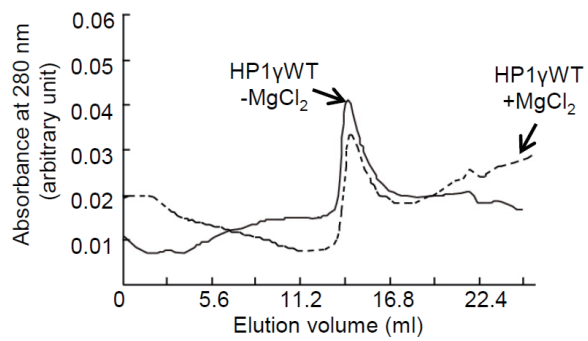
Supplementary Figure S3



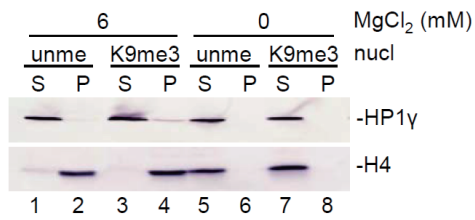
Supplementary Figure S4



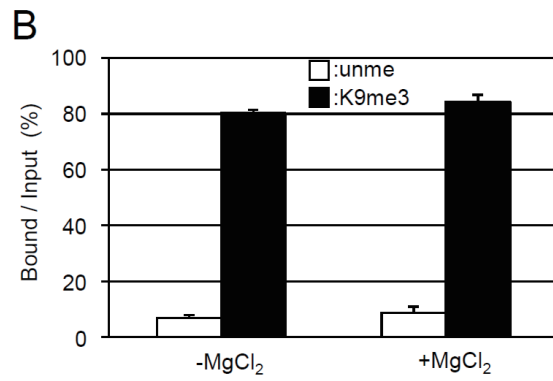
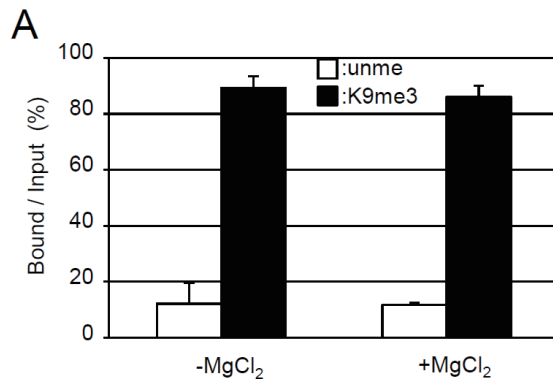
Supplementary Figure S5

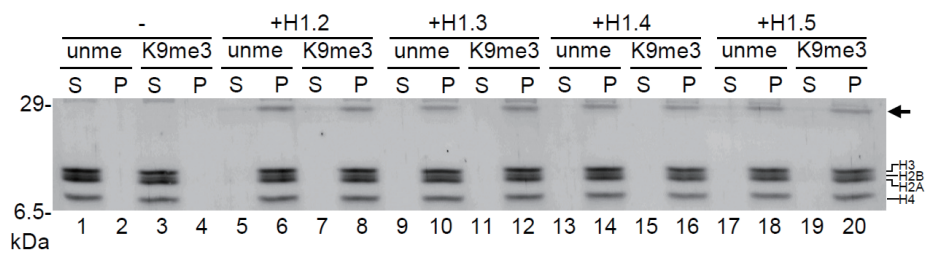


Supplementary Figure S6

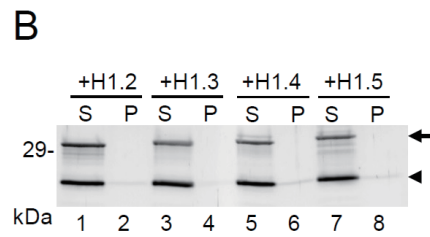
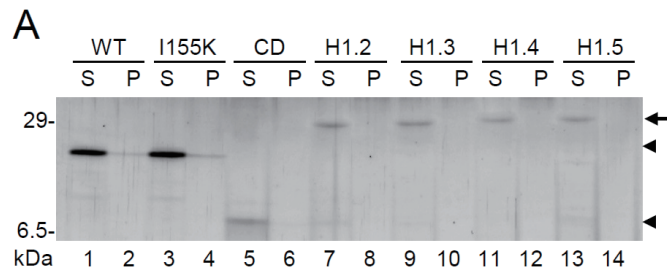


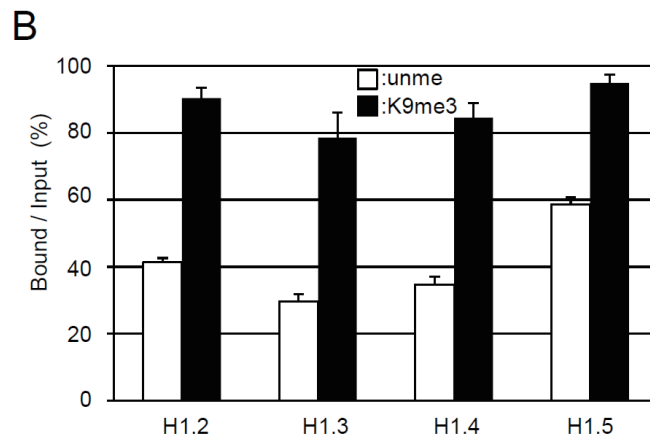
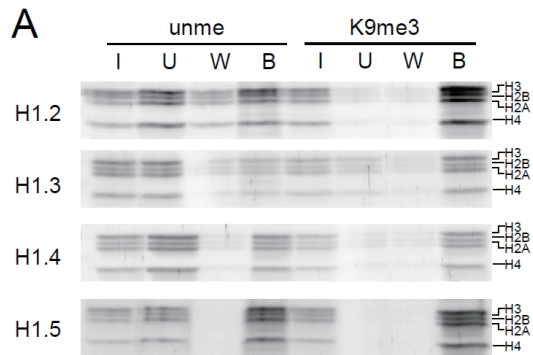
Supplementary Figure S7

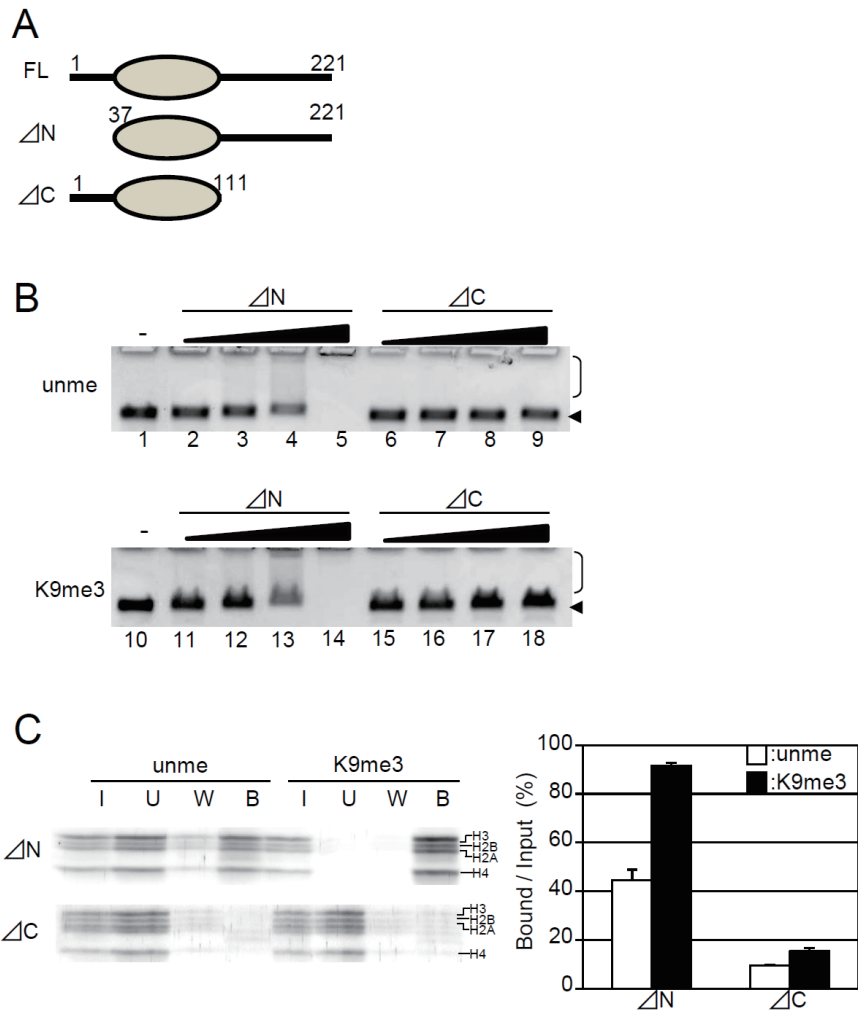




Supplementary Figure S9







Supplementary Figure S12

Fig. 1A

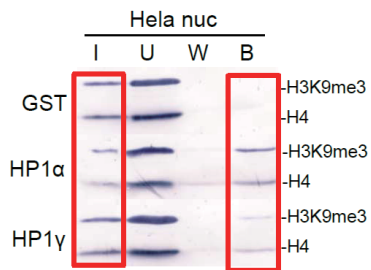


Fig. 1C

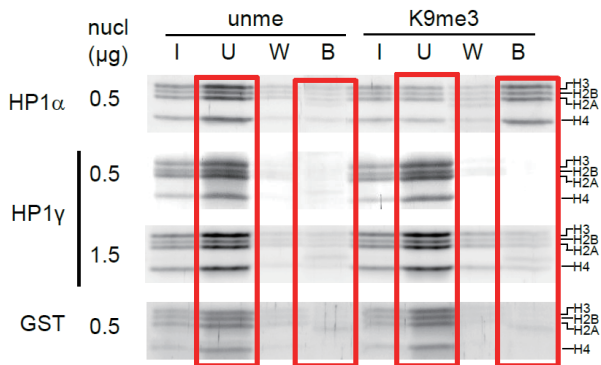


Fig. 1G

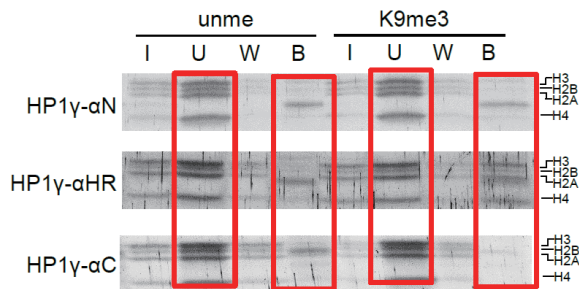


Fig. 2A

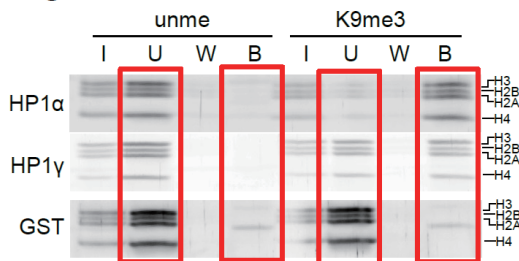


Fig. 2C

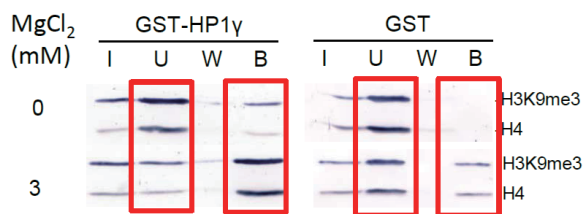


Fig. 2E

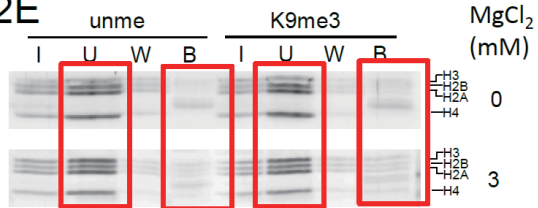


Fig. 3B

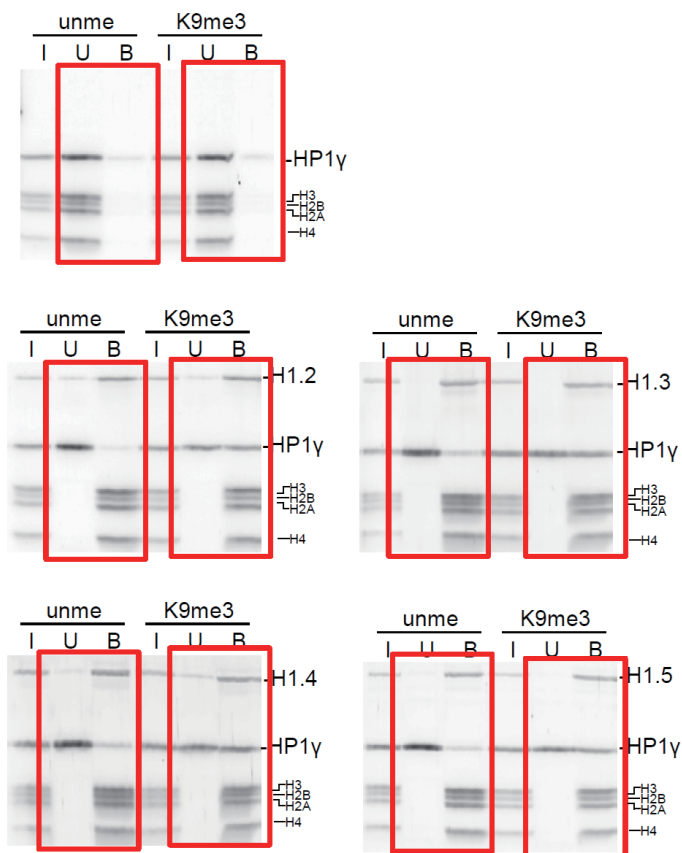


Fig. 4A

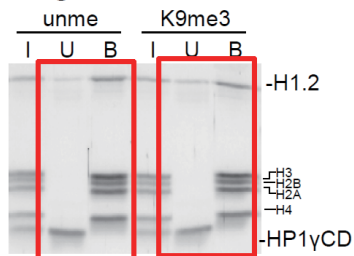


Fig. 4C

